AC/AC Converter Flexibly Connects AC Microgrid with Integrated Storage System

Nguyen Van Dung[1] and Nguyen The Vinh[2,*]
[1] School of Electrical and Electronic Engineering, Hanoi University of Industry, Hanoi City, Vietnam
[2] Faculty of Electronic Engineering I, Posts and Telecommunications Institute of Technology Hanoi, Vietnam
Email: Dungnv@haui.edu.vn (N.V.D.), vinhnt@ptit.edu.vn (N.T.V.)

Manuscript received September 6, 2025; revised October 13, 2025; accepted November 5, 2025
*Corresponding author

***Abstract*—A more stable grid is achieved by storage systems, with Alternating Current (AC) microgrids providing more continuous grid operation by supplying energy to electrical loads from distributed energy sources and energy sources from the old distribution grid. The article provides specific content of a three-port converter that connects distributed energy sources (renewable energy sources), storage systems to the AC microgrid. The converter uses Direct Current (DC) Sinusoidal Pulse-Width Modulation (SPWM) with the design foundation of Direct Current/Direct Current (DC/DC) energy converters such as H-bridge and Buck-Boost. It aims to realize the operation of a microgrid system that provides more continuous and stable power to the system when operating independently and connected to the main grid. The results of the whole project are verified by simulation and experiment with the power value of 2-5.5kW achieving an average efficiency of each case together close to 97% and are compared with some reference documents.**

***Index Terms*—Alternating Current/Alternating Current (AC/AC) converter, Alternating Current (AC)/ Direct Current (DC) converter, energy storage, bi-directional converter, microgrid**

I. Introduction

In the process of developing distributed energy sources, as well as the load stability in microgrids and integration into the main power grid [1, 2], the use of power electronic converters has many advantages, such as increasing the continuity of power supply of power to the distribution grid, the ability to improve efficiency in the conversion process, and combining components in the system with the ability to intelligently integrate with the modern power grid [3, 4]. Reducing emissions to the environment, saving fossil energy by using electric vehicles [5], proposals to increase the stability of the power system, and improving the quality of power from self-generated microgrids through power electronic converters connecting multiple inputs and outputs such as [6–9]. Moreover, the contributions of power electronic conversion technologies for wireless power transmission have been continuously improved for mobile loads such as electric vehicles and mobile phones [10, 11] to save transmission lines and make the connection of the power system safer and more convenient.

The principle of Alternating Current/Alternating Current (AC/AC) converters is implemented using electronic switching components that perform basic control according to the sinusoidal pattern of the AC source parameters [12], without the ability to increase the voltage, and the output frequency is not flexibly adjusted. The proposed studies on AC/AC converters, which apply the principles of basic Direct Current/Direct Current (DC/DC) converters [13, 14] using Pulse Width Modulation (PWM) control method to increase and decrease the output voltage, however, the energy conversion is unidirectional, the conversion capacity is limited, the basic components used are basic DC/DC converter circuits, bidirectional converters are isolated as electronic transformers [15] cannot be connected to the storage system. Several studies on direct AC/AC converters employing principles such as Boost and Buck have achieved quite high efficiency with a negligible reduction in the number of switching components; however, these studies were only performed at low power [16–20]. The AC/AC converter has two power conversion structures, one straight conversion in one stage AC/AC and two-stage AC/DC/AC conversion through an intermediate stage generating DC energy, performing two forms of rectification and inversion conversion, resulting in the control being performed in two different processes, without connecting the storage system for flexible operation and optimal performance of the converter [21, 22]. The DC intermediate stage uses a stabilized capacitor bank, which is a problem that increases the size and number of components for the converter [23]. The connection to a storage system to increase system stability and shorten the conversion time, and the continuity of power supply to the load by supercapacitors and batteries in distributed power systems but using multiple independent converters to perform operation [24]. Some applications use AC/AC power transmission technology without a DC intermediate stage by power electronics such as electronic transformers for transmission for microgrids and main grid connection [25, 26], which limits operational flexibility and uninterrupted power supply and inefficient use of distributed energy resources.

This research introduces a single-stage AC/AC converter designed for flexible bidirectional operation and compact single-phase implementation with integrated energy storage. A key objective is to minimize leakage energy during the main switching process, thereby

doi: 10.18178/ijeetc.15.1.44-52

reducing switching losses, as illustrated in Fig. 1. The converter utilizes two single AC switches and one switch for the energy storage system, as shown in Fig. 2, which simplifies both construction and control. An oscillator-based control technique eliminates switching current and precisely regulates resonant current. Additionally, this work provides a comprehensive review of AC/AC converter topologies, including AC choppers and systems with or without integrated storage.

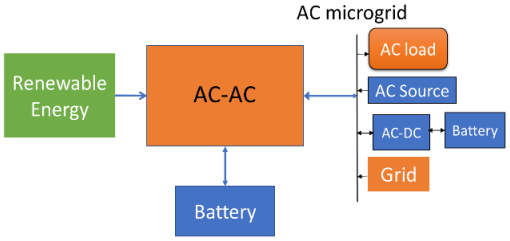

Fig. 1. Block diagram of AC microgrid connection with renewable energy source integrated with storage system.

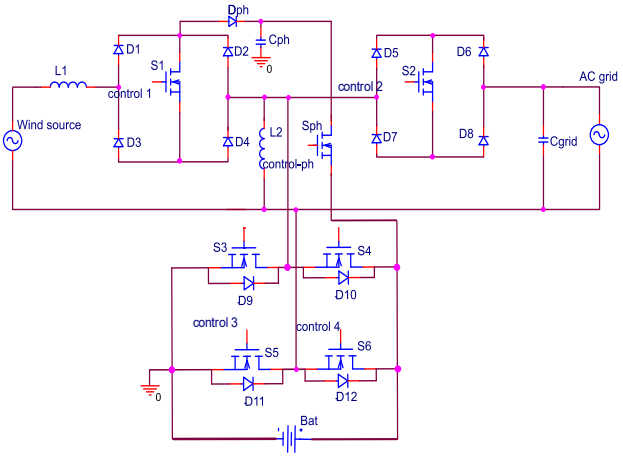

Fig. 2. Proposed AC/AC converter circuit with storage.

II. AC/AC-Storage Converter

The proposed converter circuit is shown in Fig. 2. In this converter, two main switches (S1 and S2) are used to convert energy from wind power to the AC microgrid, while eight auxiliary switches are implemented as diodes D1-D8. Four additional switches (S3–S6) form an H-bridge converter for the energy storage system. The soft-switching components that perform energy recovery are Sph and Dph, which are connected to the drain terminals of the two main switches, as illustrated in Fig. 2. (The figure shows a recovery circuit connected to switch S1; a similar soft-recovery circuit is connected to switch S2.). In this converter, the Dph and Cph energy recovery circuits are used to connect the recovery energy to the energy storage system during the energy conversion process. In the simple connection circuit and multi-case operation to create a continuous power supply for the AC microgrid load, using the optimal energy for renewable energy sources. Integrated converter for another AC microgrid.

The AC microgrid connected to the direct-conversion power converter with an integrated storage system operates under the following cases.

Operating Mode 1 and Mode 2 of Case 1 are shown in Fig. 3. In this case, energy is supplied only from the wind power source to the AC grid when the energy storage system is fully charged and the AC microgrid load increases, requiring additional energy. The converter works as a buck-boost DC converter. In Mode 1 of operating Case 1, energy is transmitted directly from the wind power source to the AC grid through the switch S1 and the diodes D1 and D4, the current through the coils L_1 and L_2 in the time period equal to the opening time of S1 in the control cycle for S1 is d1 (duty cycle), in the power circuit there is an integrated energy recovery circuit at the drain pole of S1, S2. This circuit aims to reduce voltage and current spikes across S1 and S2, thereby limiting switching losses during the energy conversion process. This mode converter is not linked to the storage system, and the storage is not active. During the interval $d_1 \in (0, \pi)$, corresponding to Mode 1, the main switch S1 is turned on. The current flowing through switch S1 and inductor L_2 is equal to the current in inductor L_1. Meanwhile, the main switch S2 is turned off, and the AC microgrid is supplied by energy stored in capacitor Cgrid.

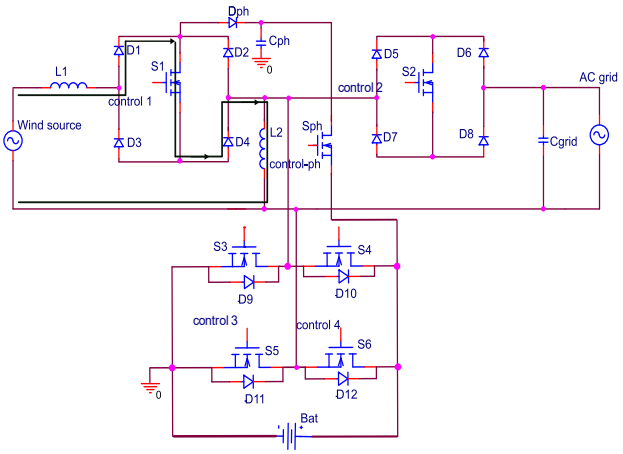

(a)

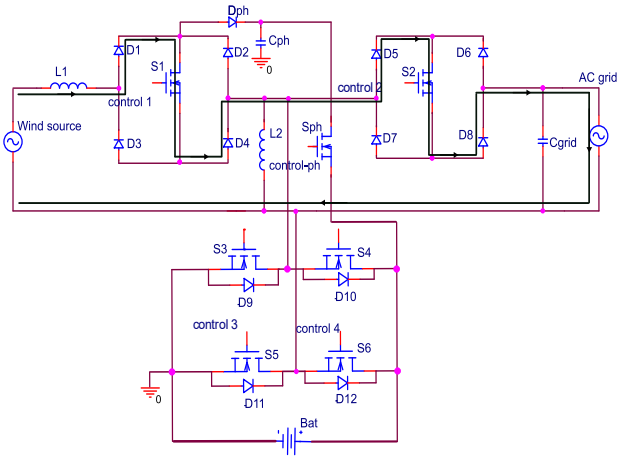

(b)

Fig. 3. Operation modes of the proposed converter in Case 1: (a) Mode 1 and (b) Mode 2.

During the time d_2 (duty cycle) of S2 is in (0-π) is Mode 2, d_2 is the delay time to turn on S2 after S1. In Mode 2 switches S1 and S2 turn on, diodes D1, D4, D5, and D8

turn off, grid-connected capacitor Cgrid is charged, and grid energy received from the wind power source. Mode 2 belongs to time period (0-π). Energy is transferred from the wind power source to the AC microgrid load through the switching process of the main switches and diodes. In this converter, the control principle is used as a DC/DC converter. During Mode 2, inductor L_2 continues to store energy via switch S1 and diodes D1 and D4, transferring it back to the wind power source as in Mode 1. Capacitor Cgrid remains charged.

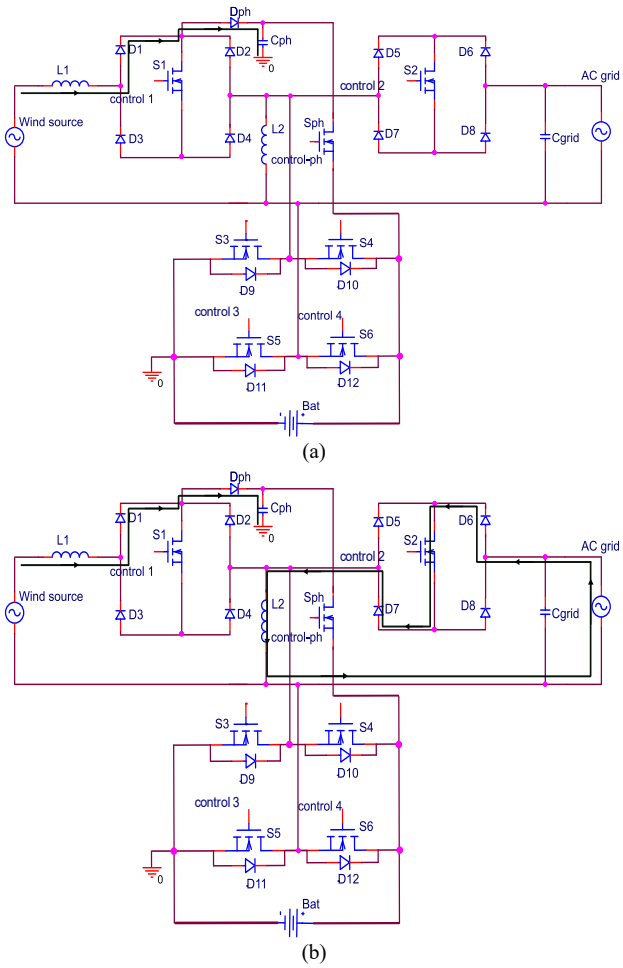

Fig. 4. Operation modes of the proposed converter in Case 1: (a) Mode 3, (b) Mode 4.

Mode 3: When S1 is turned off, S2 is turned off, energy is supplied to capacitor Cph through D1 and Dph because the voltage at cathode Dph is more positive than anode as shown in Fig. 4 (a), the Sph switch does not operate in this mode of Case 1. Grid energy is supplied by Cgrid.

This mode is performed during the time when there is no pulse to S1 and is determined from a constant depending on the value of capacitor Cph and the parameters of diodes Dph and D1 as in the expression (1):

$$\tau = (R_{D1} + R_{\text{Dph}})\text{Cph} = \frac{1}{2\pi f_{\text{SW}}} \quad (1)$$

where τ is the time constant for charging of capacitor Cph; f_{sw} is switching frequency of S1; R_{D1} is the internal resistor when diode D1 conducts; and R_{Dph} is the internal resistance of diode Dph when conducting current.

The expression will determine less than or equal to the time when there is no pulse of S1.

Mode 4: When S1 is locked, S2 is open, AC grid energy is still supplied by Cgrid as shown in Fig. 4 (b), recovery energy still charges Cph through D1 and Dph. Recovery energy will charge the storage in a shorter time than the time S1 is open in this mode. The converter operation returns to Mode 2. The energy stored in inductor L_2 is supplied to the microgrid load through the main switch S2 and diodes D6 and D7.

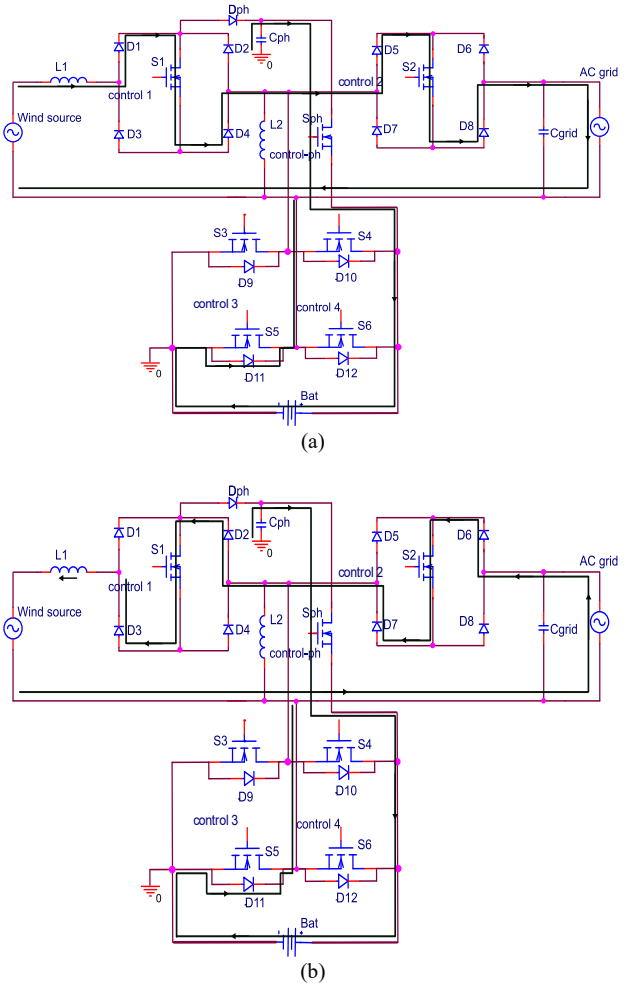

Fig. 5. Operation modes of the proposed converter in Case 1: (a) Mode 5, (b) Mode 6.

Case 1 of the converter has the operating modes in the 0 to π period described in detail in Mode 1 to 4, the operations have additional modes of the energy recovery circuit Mode 3 and Mode 4. In addition, the converter has modes similar to the 0 to π half-cycle operation, then the π to 2π half-cycle as described in Fig. 5 shows when the main switches S1 and S2 change state and the switch S2 operates mainly with the recovery circuit connected to the drain pole as the recovery circuit at switch S1 to voltage stress limitation on switch S2. The leakage energy is also performed as Modes 5 and Mode 6 as shown in Fig. 5 (a) and Fig. 5 (b) by controlling the switch Sph. Besides, together with the energy from the wind power source to the load. The leakage energy of the coils L_1 and L_2 is calculated as expressions (2), (3) and (4) suitable for selecting the

parameters of Dph and Cph to ensure effective recovery properties for the storage system and limit the loss on the main switch S1 and S2.

$$L_1 = \mu_0 \mu_r \frac{N^2 r^2}{D} \quad (2)$$

where μ_0 is the permeability of vacuum; μ_r is the relative permeability of core material; N is the number of turns of the inductor L_1; r is the winding radius (m) of the inductor L_1; and D is the ring diameter (m) of the inductor L_1.

$$W_{\text{leakage}} = \frac{1}{2} L_1 \times i^2(t) \quad (3)$$

where i is the current flowing through coil L_1 and switch S1.

The leakage energy of coil L_1 depends on the switching frequency variation current of switch S1.

$$V_{L_1} = -L_1 \frac{di}{dt} \quad (4)$$

The voltage on the storage system is selected to calculate so that the value will be less than the impulse voltage value when the switch S1 or S2 operates to change the state from open to locked, which is 235VDC. This reason is to give the condition to choose the storage system and manage the connection to match the voltage and current values of Bat to accumulate energy effectively from distributed energy sources and recovery energy.

Input parameters in the simulation process by Orcad software for the converter are shown as wind power source: stable output voltage 220V, 50Hz; maximum output power 10kW; stable ideal wind speed. AC microgrid: Effective voltage 220V, fluctuation +5V; load fluctuation in the range of 2-6kW; power generated from the grid 2-5kW. Storage system: charging and discharging fluctuation power 2-5kW. The simulation graph of Mode 1 to Mode 4 in Case 1 is shown in Fig. 6. The current through S1 changes a lot during the positive half-cycle amplitude period, and the change increases with the opening and closing time value of the switch S1. It shows the transient process in the energy conversion process that affects the selection of the switch corresponding to the current. The control switching frequency corresponds to 20kHz. The current and voltage graphs from the wind power source and the AC microgrid are basically stable and similar to a sinusoid with a frequency of 50Hz. The transmitted energy from the wind source has a value of more than 6kW. This case can be performed in the opposite direction of transmitting energy from the AC microgrid to the source side if we replace the wind power source with an AC microgrid. This converter can perform bidirectional operation with the same principle.

Similar to the switching frequency control circuit as in Mode 1 to Mode 4. The graph in Fig. 7 shows the current and voltage values represented on switch S1 and additionally shows the recovered energy value supplied to the storage system. Mode 5 and Mode 6 of Case 1 represent the energy value recovered by the recovery circuit Cph, Sph, which charges the storage system when the main switch S1 switches from turned on to turned off. The voltage on switch S1 is limited to a maximum compared to the basic voltage fluctuations of the input source as shown in Fig. 7. In the converter when the energy direction is transferred from the AC microgrid to the wind power source when replaced by an AC microgrid, the charge recovery circuit on the main switch S2 works as the analysis modes on the recovery circuit connected to the switch S1.

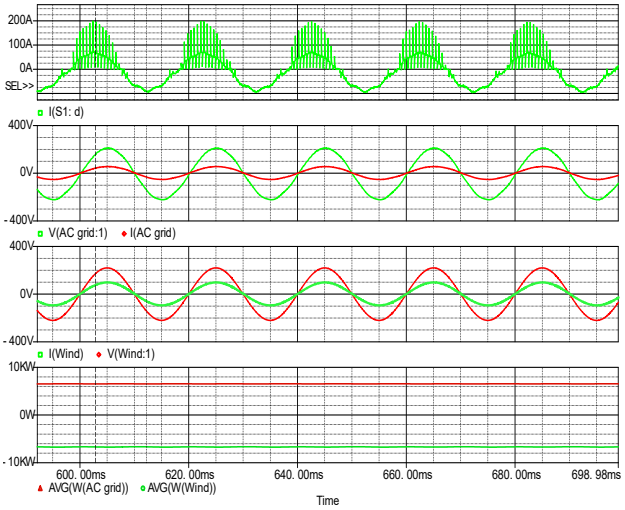

Fig. 6. Simulation results of the proposed converter in Case 1 operated in Mode 1 to Mode 4.

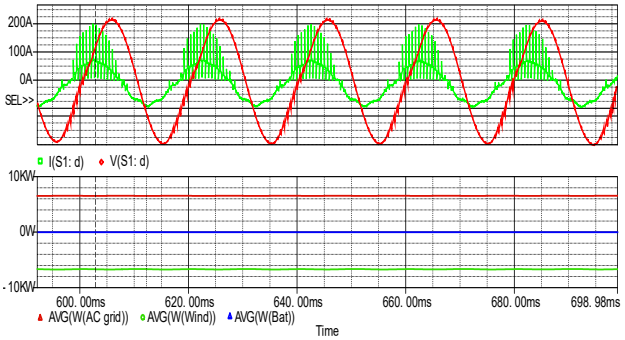

Fig. 7. Simulation results of the proposed converter in Case 1 operated in Mode 5 and Mode 6.

Case 2 describes the operation as shown in Fig. 8 (a), the energy storage system receives energy from the renewable energy source (wind) and the energy from recovery circuit energy Dph, Cph during switching of key S1. This energy is collected during energy conversion operations. This recovery energy has a small value to accumulate excess energy from the opening and closing process with the energy of the inductor L_1. The voltage when the capacitor Cph is fully charged will be greater than the voltage on the drain pole of S1, at this time the energy is discharged to the storage system. The AC grid energy is still supplied from the wind power source by the same operation as Case 1.

The simulation results of Case 2 are shown in Fig. 8 (b) with the current and voltage waveforms of the wind power source and the AC grid. The input voltage signal of the storage system with a simulated value of nearly 225VDC, at this time the leakage energy accumulated in the Cph capacitor is discharged to the storage system. And the power values at the wind power sources, the AC microgrid loads and the Bat storage system. When the storage system

reaches the standard voltage and is fully stored, the Sph recovery switch does not work, the S3-S6 switches do not work. Energy is only supplied to the AC microgrid loads. This is an undesirable operating mode because the energy of the storage system is not always full.

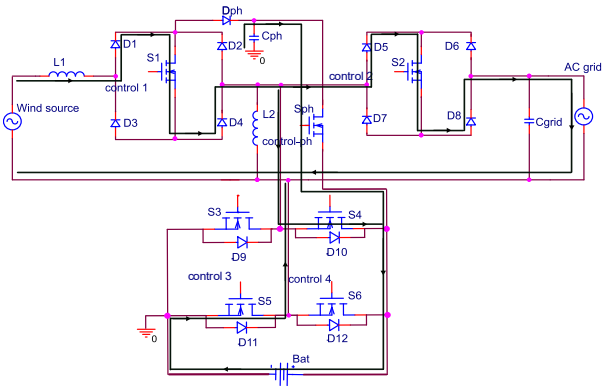

(a)

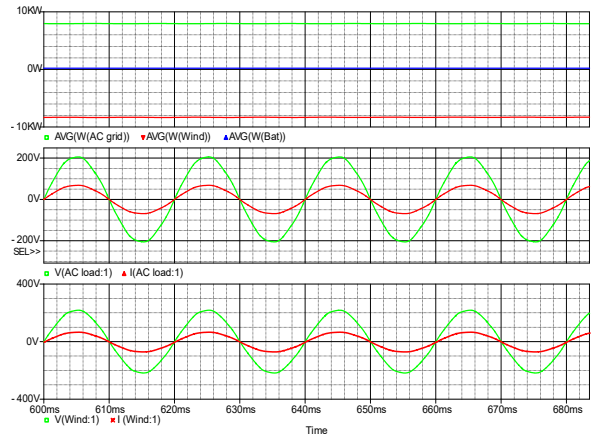

(b)

Fig. 8. Operation of the proposed converter in Case 2: (a) Circuit diagram and (b) simulation results.

Case 3, illustrated in Fig. 9, occurs when the AC microgrid is supplied entirely by the energy storage system. In this situation, wind power cannot generate electricity due to environmental constraints, and other sources are unable to meet the load demand. The converter functions as an H-bridge inverter, with switch S2 operating bidirectionally in each half cycle of the AC grid voltage. Power switch S1 is inactive. The recovery circuit at switch S2 operates with Sph control.

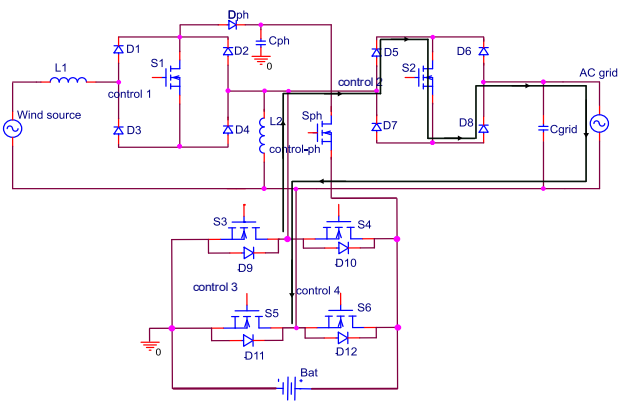

(a)

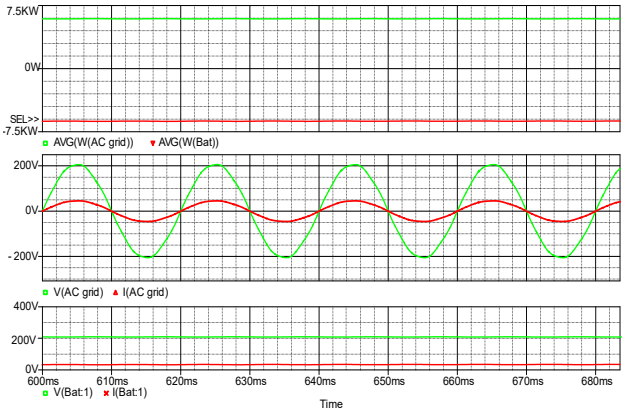

(b)

Fig. 9. Mode 6 operation of the proposed converter in Case 3: (a) Circuit diagram and (b) simulation results.

The simulation results are depicted in Fig. 9 (b), with the voltage current quality to the AC microgrid and from the storage system being quite good with frequency and voltage amplitude matching the distribution grid. The converted power with a value greater than 7kW to the AC microgrid load. The recovery power is still received from the recovery circuit to the storage system to save and limit the voltage stress on switch S2.

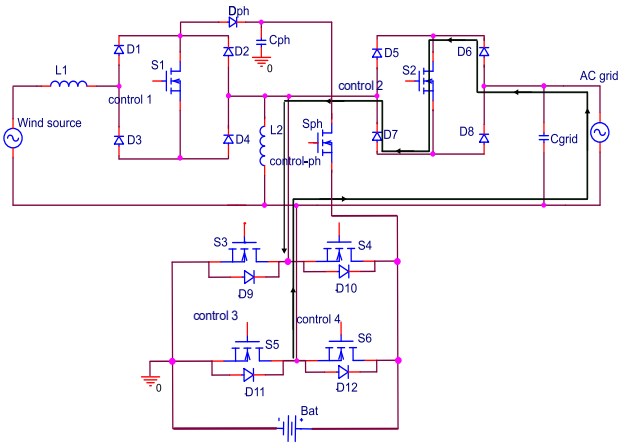

(a)

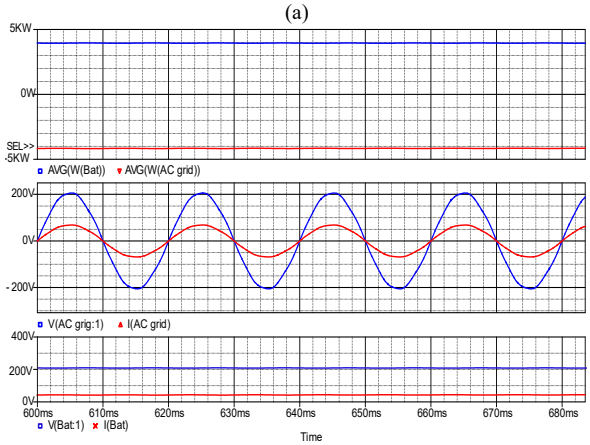

(b)

Fig. 10. Operation of the proposed converter in Case 4: (a) Circuit diagram and (b) simulation results.

Case 4, illustrated in Fig. 10 (a), corresponds to the condition in which the storage system is charged by the AC microgrid. This situation occurs when the wind power

source is stopped, and excess energy is available from the distributed power sources in the microgrid. In this case, the converter functions as a single-phase bridge rectifier. The recovery circuit connected to the main switch S2 operates during the switching interval, recovering the leakage energy stored in inductor L_2 and reducing the voltage stress across S2.

The energy is supplied by the main switch S2 and the switches S3-S6 in the H-bridge. The converter is capable of increasing the voltage value to 230VDC to meet the ability to receive energy from the single-phase AC microgrid. The charging process determines the power value depending on the load power value, the power source, and the storage system in the AC microgrid, as shown in expression (5). Besides, the recovery circuit works and still provides some power to the storage system as in case 4.

$$P_{\text{source AC grid}} > P_{\text{AC\_load}} + P_{\text{AC\_bat}} \quad (5)$$

Fig. 10 (b) shows the operation graph of Case 4 with the current and voltage values of the AC grid and the storage system. The average voltage on the storage system is 225VDC, the voltage from the AC microgrid is 220VDC. The transmission power has a simulated value of more than 4kW. In this simulation result, the current and voltage quality between the input and output of the converter are guaranteed with a control switching frequency of 20kHz.

As shown in Fig. 11, Case 5 represents the condition in which energy from the wind source is used to charge the storage system. This occurs when the AC grid load is fully supported by internal distributed sources. In this configuration, switch S1 and switches S3–S6 form a rectifier, and the recovery circuit operates in the same manner as in Case 1 (Mode 3 and Mode 4). The control strategy includes a power point tracking algorithm for the wind source, while the recovery circuit mitigates voltage stress on switch S1.

The transmitted energy has a value of more than 8kW. The current and voltage forms from the wind power source and the storage system are shown in Fig. 11 (b). The average voltage on the storage system is 225VDC, the voltage and current are sinusoidal with a frequency of 50Hz, the effective value is 220V, and the energy conversion quality is stable. The recovered energy also partially recharges the storage system in this case.

The control technique proposed in the paper is the sinusoidal PWM (SPWM) control. Fig. 12 shows the control diagram implemented with 4 main cases in the operation of the proposed converter. Case 1 and Case 2 are controlled by the same control method. The remaining Case 3 to Case 5 are different. Each control method is shown in the block diagram by the PWM control method for AC/AC bidirectional power conversion and SPWM for DC/AC and AC/DC conversion, respectively, according to the operating principle of the converter. In Case 1 and Case 2 the converter operates on the buck-boost converter principle implemented with SPWM DC modulation, with an integrated energy recovery circuit. During one cycle of the alternating current. Voltage and power current feedback signals are taken from the AC microgrid inputs and the DC storage system.

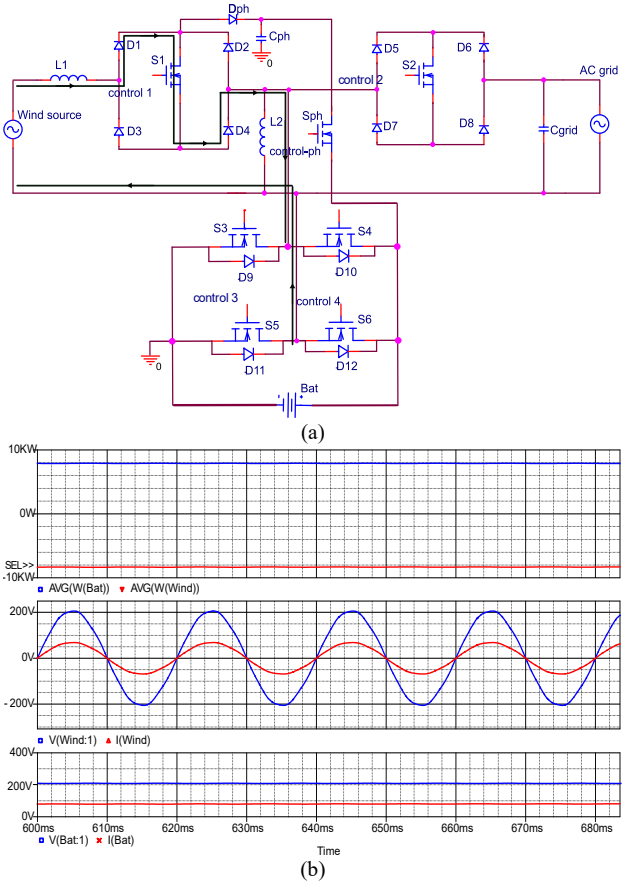

Fig. 11. Operation of the proposed converter in Case 5: (a) Circuit diagram and (b) simulation results.

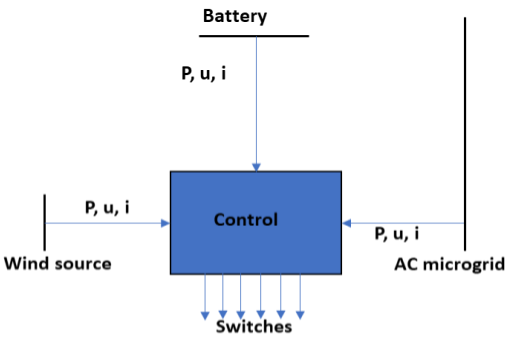

Fig. 12. Converter control diagram.

III. Experimental Discussion

Fig. 13 illustrates the experimental prototype of the AC/AC converter, showing the actual components used in the AC microgrid and renewable energy systems. Laboratory experiments were performed at power levels ranging from 2.5 to 5.5 kW. The detailed input parameters for the prototype are provided in Table I. These experimental values were selected based on the theoretical analysis and simulation results, ensuring consistency with the simulated operating range.

The experimental values of voltage, current, and power of the wind power source in the laboratory supply to the AC microgrid load and the storage system with different actual values from 1.2–5.4kW. The experimental system in the process of adjusting the actual power value with the

input parameters from Table I shows that the power only reaches nearly 5.5kW during the energy conversion process in each case as shown in Fig. 14 (a). The reason is that the power of the switch does not meet the simulated conversion capacity. As Fig. 14 (b) shows, the power of the storage system is transmitted to the AC microgrid load.

TABLE I: EXPERIMENTAL PARAMETERS OF THE PROPOSED CONVERTER

Input parameters, equipment	Value/code
Output voltage of wind power source	220VAC
Wind power source frequency	50Hz
Wind power source capacity	1-5,5kW
AC microgrid load	2-5kW
AC microgrid parameters	220VAC, 50Hz
Voltage on storage system	225VDC, 12Ah
Diodes	SBR40U300CTB-13
Diode Dph	SBR20A300CT
Switchs S1-S6	150EBU04
Coils L_1, L_2	10μH, 10mH
Capacitor Cgrid	100μF

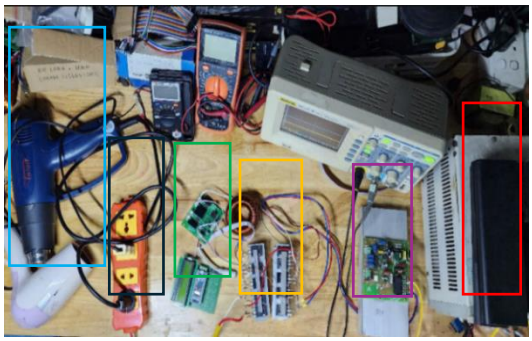

Fig. 13. Proposed AC/AC converter image, black frame shows AC grid, purple frame shows wind power, red frame shows storage system, orange frame shows converter, green frame shows controller, blue frame shows AC grid load.

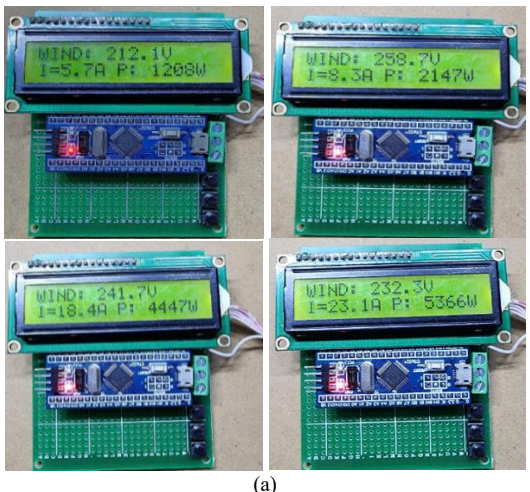

(a)

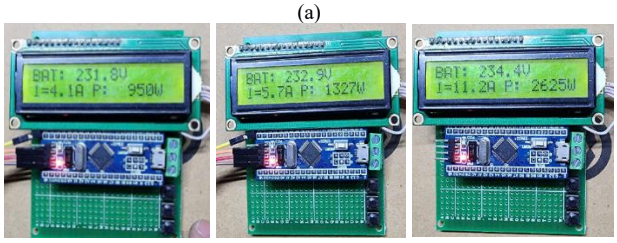

(b)

Fig. 14. Experimental image of the converter in the laboratory: (a) Measure the current, voltage and power parameters of the wind power source and (b) measure the current, voltage and power of the storage system.

Fig. 15 (a) shows the wind power source voltage (yellow) with a sinusoidal shape with parameters meeting the input parameters given in Table I and the AC microgrid voltage (blue), as shown by the experimental signal having some non-standard waveform segments corresponding to the simulation results when the recovery circuit is not working effectively leading to high oscillation of the switching voltage on the switch affecting the quality of the AC microgrid output voltage. Fig. 15 (b) the voltage on switch S1 during SPWM modulation in Case 1 operation of the proposed converter.

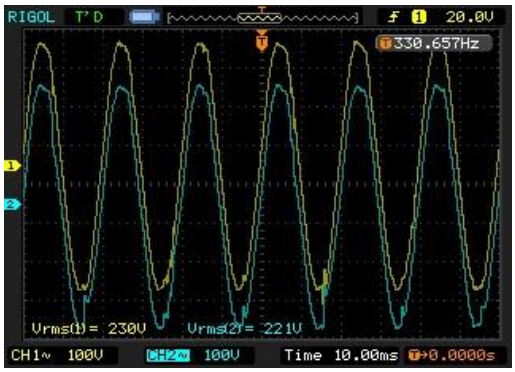

(a)

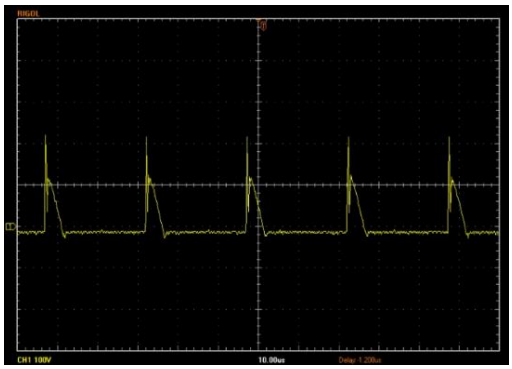

(b)

Fig. 15. Actual signal shape at 5kW load power, switching frequency for 20kHz switches in the Case 1: (a) voltage on the grid (blue) and wind power source (yellow) and (b) voltage on switch S1.

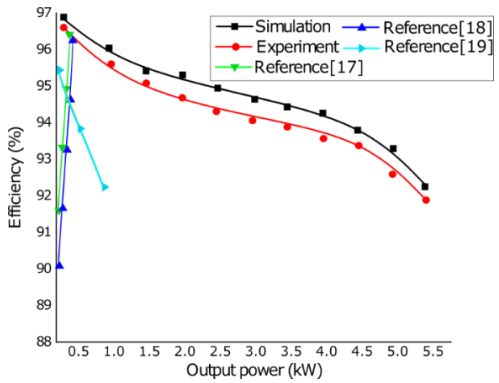

Fig. 16. Proposed converter performance comparison.

The calculated simulation results give the average efficiency of each case in the converter, Case 1 to Case 5 is depicted in Fig. 16. The efficiency value in the power range less than 2kW, the efficiency of the proposed converter is larger than the efficiency of the converter

in [17, 18] by more than 6%. For the value greater than 2kW, the efficiency value of the proposed converter decreases gradually with each power value until 5kW, the experimental efficiency is nearly 92%. This value compared to the converter efficiency [19] is almost equal to 92.3% with 1kW corresponding to the output power value of the load at the AC microgrid and the storage system.

IV. Conclusion

The experimental results of the proposed converter demonstrate that it satisfies key practical requirements for energy conversion in AC microgrids. It enables efficient power transfer from distributed renewable energy sources and storage systems, thereby reducing dependence on fossil-fuel-based power generation. The converter ensures high-quality power conversion for both storage systems and microgrid loads at a capacity of 5.5 kW. Its structure is simple, with a reduced number of components in the power circuit, resulting in high efficiency, ease of control, and improved system stability. Moreover, the converter's capacity can be expanded by parallel connection within the microgrid when multiple distributed energy sources are available. It can also interconnect two or more grids if additional conversion ports, similar to those used for wind power connections, are integrated into the circuit. Overall, the proposed converter can be readily incorporated into smart grid systems at regional or national scales.

Conflict of Interest

The authors declare no conflict of interest.

Author Contributions

Nguyen Van Dung drafted the manuscript and contributed to the hardware design and development. Nguyen The Vinh was responsible for developing the hardware setup, software implementation, and obtaining the results and responsible for conceptualizing the idea, providing guidance, and supervising the research. All authors reviewed and approved the final version of the manuscript.

Acknowledgment

The research team would like to thank the Posts and Telecommunications Institute of Technology Hanoi, Vietnam for creating favorable conditions during the implementation of the research content of this article.

References

[1] O. M. Neda, "Hybrid design of optimal reconfiguration and DG sizing and siting using a novel improved salp swarm algorithm," *Electr. Eng.*, vol. 107, pp, 14159–14174, 2025. https://doi.org/10.1007/s00202-024-02493-7

[2] O. M. Neda, "Optimal amalgamation of DG units in radial distribution system for techno-economic study by improved SSA: Practical case study," *Electric Power Systems Research*, vol. 241, 111365, 2025. https://doi.org/10.1016/j.epsr.2024.111365

[3] A. Anvari-Moghaddam, P. Davari, and O. Hegazy, "Power electronic applications in power and energy systems," *Applied Sciences*, vol. 13, no. 5, 2023. https://doi.org/10.3390/app13053110

[4] N. T. Vinh and N. V. Dung, "Bidirectional AC/AC converter linking two microgrids in a flexible microgrid," *International Journal of Power Electronics and Drive System*, vol. 16, no. 1, pp. 389–406, 2025.

[5] H. Li, H. Li, Y. Hu, T. Xia, Q. Miao and J, Chu, "Evaluation of fuel consumption and emissions benefits of connected and automated vehicles in mixed traffic flow," *Front. Energy Res.*, vol. 11, 1207449, 2023.

[6] O. M. Neda, "A review on smart distribution systems and the role of deep learning-based automation in enhancing grid reliability and efficiency," *Buletin Ilmiah Sarjana Teknik Elektro*, vol. 7, no. 2, pp. 195–205, Jun. 2025.

[7] P. N. Thang, V. T. Vinh and N. T. Vinh, "A flexible DC-DC converter for the Battery-DC bus renewable energy system," *International Energy Journal*, vol. 20, no. 4, pp. 581–594, 2020.

[8] F. Li, D. Wang, D. Liu, S. Yang, K. Sun, Z. Liu, H. Yu, J. A. Qin, "Comprehensive review on energy storage system optimal planning and benefit evaluation methods in smart grids," *Sustainability*, vol. 15, no. 12, 9584, 2023.

[9] S. M. Rashid and A. R. Ghiasi, "Power management enhancement and smoothing DC voltage using integrated BESS and SMES in Off-grid hybrid AC/DC microgrid based on ILCs," *Sci. Rep*., vol. 15, 2025. https://doi.org/10.1038/s41598-025-07873-y

[10] B. Latha, M. M. Irfan, B. K. Reddy *et al.*, "A novel enhancing electric vehicle charging: An updated analysis of wireless power transfer compensation topologies," *Discov. Appl. Sci*., vol. 240, 2025. https://doi.org/10.1007/s42452-025-06630-0

[11] M. T. Tran, S. Thekkan, H. Polat *et al.*, "Inductive wireless power transfer systems for low-voltage and high-current electric mobility applications: review and design example," *Energies*, vol. 16, no. 7, 2953, 2023.

[12] D. S. Rosas, D. Chavez, D. Frey, and J-P. Ferrieux, "Single-stage isolated and bidirectional three-phase series-resonant AC–DC converter: Modulation for active and reactive power control," *Energies*, vol. 15, no. 21, 8070, 2022.

[13] I. Abdoli, M. K. Hajiabadi, A. Mosallanejad, L. A. Eshkevari, "A single-phase P-type AC-AC converter with reduced components count and high boost factor," *Int. J. Circ. Theor. Appl.*, vol. 51, no. 1, pp. 360–378, 2023.

[14] K. Nandakumar, V. Mohan, F. Alsaif *et al.*, "Design and analysis of solitary AC–AC converter using reduced components for efficient power generation system," *Sci. Rep.*, vol. 14, 9323, 2024.

[15] H. Wang, S. Xie, and L. Yuan, "A single-phase AC-AC power electronic transformer without bulky energy storage elements," *Energies*, vol. 18, no. 7, 1769, 2025.

[16] H. F. Ahmed, C. H. Chung, A. A. Khan, Z. Aleem, F. Akbar, O. Alzaabi, "Nondifferential AC choppers based identical bipolar buck-boost AC-AC converter without commutation issue," *IEEE Trans. Power Electron*., vol. 38, no. 4, pp. 4988–4999, 2023.

[17] G. Dong, S. Liu, T. Mishima, and C.-M. Lai, "Fixed-off-time pulse coding modulation for single-phase resonant direct AC-AC converter in high-frequency induction heating systems," in *Proc. 2024 IEEE Energy Conversion Congress and Exposition*, Phoenix, USA, 2024. doi: 10.1109/ECCE55643.2024.10861800

[18] H. F. Ahmed, A. L. Eshkevari, and I. Abdoli, "An identical bipolar buck-boost AC-AC converter based on a coupled-inductor with safe-commutation, high gain, and high efficiency," *IET Power Electron.*, vol. 17, pp. 3005–3016, 2024. https://doi.org/10.1049/pel2.12818

[19] D. Shahzad, S. Pervaiz, N. A. Zaffar, and K. K. Afridi, "GaN-based high-power-density AC–DC–AC converter for single-phase transformerless online uninterruptible power supply," *IEEE Trans. on Power Electronics*, vol. 36, no. 12, pp. 13968–13984, Dec. 2021.

[20] E. Sztajmec and P. Szcześniak, "A review on AC voltage variation compensators in low voltage distribution network," *Energies*, vol. 16, no. 17, 6293, 2023.

[21] D. Guo, A. Wang, C. Liu *et al.*, "Novel bidirectional high-frequency isolated direct AC/AC converter with unipolar phase-shifted modulation strategy," *IEEE Trans. on Power Electronics*, vol. 39, no. 2, pp. 2644–2659, Feb. 2024.

[22] S. M. J. Mousavi, E. Babaei, M. Sabahi, and H. Komurcugil, "A class of bidirectional single-phase Z-source AC–AC converter with continuous input current and reduced component count," *IEEE Trans. on Power Electronics*, vol. 38, no. 5, pp. 6311–6318, May 2023.

[23] J. Wang, D. Q. Gao, W. Z. Shen *et al.*, "Reliability of DC-link

capacitor in pulsed power supply for accelerator magnet," *NUCL SCI TECH*, vol. 35, no. 151, 2024. https://doi.org/10.1007/s41365-024-01470-w

[24] J. I. Shuvo, M. Badoruzzaman, S. T. I. Anik, S. Ahmad, T. Ahmed, and M. Karimi, "Hybrid energy storage power management system harnessing battery-supercapacitor synergy for grid-isolated DC microgrid," *Journal of Energy Storage*, vol. 119, 116170, 2025.

[25] T. Mahmud and H. Gao, "A comprehensive review on matrix-integrated single-stage isolated MF/HF converters," *Electronics*, vol. 13, no. 1, 237, 2024.

[26] R. Gupta and Kuldeep Sahay, "AC-AC converter topologies for power applications," *J. Electrical Systems*, vol. 20, no. 3, pp. 6105–6119, 2024.

Nguyen Van Dung was born in VinhPhuc, Vietnam. He receiced the B.S and M.S degrees in electronics engineering from the Hanoi University of Industry (HaUI), Hanoi, Vietnam, in 2009 and 2018. He is currently a lecturer at Faculty of Electronic Engineering in HaUI. His research interests include control of power electronics, control of electric drivers, smart grids, smart home and automatic control system.

Nguyen The Vinh is a lecturer in Faculty of Electronic Engineering I, Posts and Telecommunications Institute of Technology (PTIT), Hanoi, Vietnam. He graduated majoring in electrification, from Thai Nguyen University of Technology in 2001, and received his master's degree in electrical equipment, networks and power plants from Thai Nguyen University, Vietnam in 2008. He received his Ph.D. degree in electrical engineering from University of Lorraine, France in 2014. Now Dr. Vinh is the Head of Renewable Energy and Environmental Research Group. His research interests include the field of digital design, industrial applications, industrial electronics, industrial informatics, power electronics, renewable energy, embedded system, artificial intelligence, intelligent control and Embedded system for environmental measurement.